

Original Research Article

Mathematical modelling and virtual design of metamaterials for reducing noise and vibration in built-up structures

*Emmanuel C. Akaligwo¹, Anselm O. Oyem², & Olayiwola I. Babarinsa³

Affiliation

*^{1,2,3}Department of Mathematics, Federal University Lokoja, Kogi State, Nigeria

***For correspondence: email:** emmanuel.akaligwo@fulokoja.edu.ng,
tel: +234 (0) 703 492 9919

Abstract

Noise and vibration pose significant challenges in built-up structures, affecting structural integrity and occupant comfort. Traditional materials often fail to address these issues effectively across all relevant frequencies, particularly in urban and industrial environments. This paper presents a mathematical modeling approach and virtual design framework for developing metamaterials specifically tailored to mitigate noise and vibration in built-up structures. By leveraging finite element analysis, dynamic energy analysis, and optimization algorithms, the study demonstrates how metamaterials can create frequency-specific barriers. Comparative analyses with previous studies, performance metrics, and sensitivity evaluations reveal the robustness and unique contributions of this approach. Validation through simulations and benchmarking confirms the model's effectiveness, enhancing structural resilience and human comfort in complex environments. Additionally, this study surveys natural metamaterials and the urban environment. The major findings highlight the effectiveness of natural metamaterials (NMs) in ground vibration attenuation, offering diverse applications and proposing a roadmap for developing natural materials for clean and quiet environments.

Keyword: *Metamaterials, virtual design, noise reduction, built-up structures, genetic algorithm, dynamic behavior, finite element analysis*

1. Introduction

Noise and vibration are increasingly problematic in urbanized areas, impacting structural stability and human wellbeing. Built-up structures, especially those with complex geometries and mixed materials, often experience resonance effects and energy transmission across wide frequency ranges due to external sources like traffic, machinery, and environmental factors. Traditional noise and vibration mitigation methods, such as insulation or damping layers, often exhibit frequency-dependent limitations, making them less effective in low and mid frequency ranges. Metamaterials, engineered with periodic structures to exhibit unique wave interactions, provide promising alternatives by creating frequency band gaps ranges where wave propagation is significantly reduced. This study introduces a mathematical and computational framework for the design of meta materials tailored to suppress noise and vibration in built-up structures. The work also benchmarks the proposed approach against existing methods and studies, highlighting the advantages of metamaterial configurations for practical noise and vibration control. Recent advancements in metamaterials have opened new avenues for noise and vibration control, leveraging band gap creation to achieve attenuation at specific frequencies. Aumann et al., (2019)

achieved up to 15dB reduction in mid-frequency ranges with layered metamaterials, demonstrating the potential for targeted noise reduction but with limited frequency range flexibility. Zhang and Sheng, (2022) explored lightweight metamaterials in architectural applications, noting advantages in design adaptability and weight savings over traditional materials but also identifying challenges in achieving broad frequency coverage. Common examples of Mechanical metamaterials are often characterized by the type of basis structure they exhibit, figure 1. As seen in this figure, structures can be beam-based (also strut-based), plate based, or minimal surface-based.

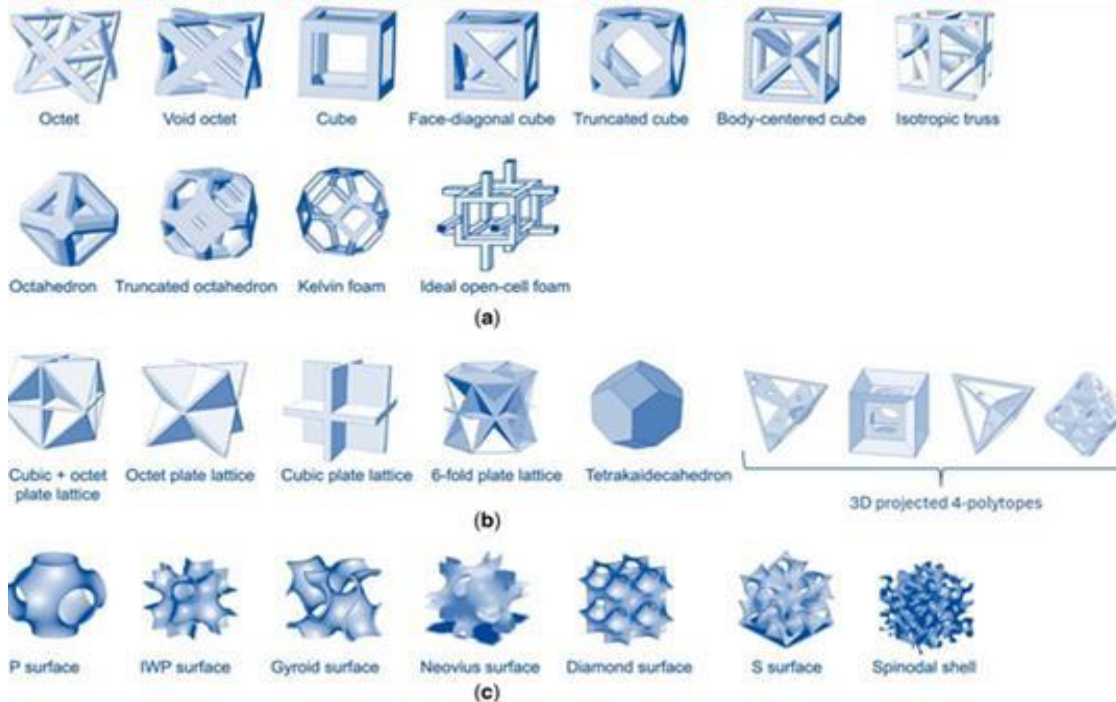


Figure 1: Examples of mechanical metamaterials based on geometry type. Illustration of 3D (a) beam-based, (b) plate-based, and (c) minimal surface-based topologies. Reprinted with the permission of [7]

Despite these advancements, many existing metamaterial designs remain constrained to narrowband applications. This study addresses these limitations by using a broader optimization framework to improve performance across a wider frequency range. Our approach integrates finite element modeling, wave propagation theory, and advanced sensitivity analysis to deliver a robust metamaterial design suitable for complex built-up environments. According to the latest statistics, more than 60% of the complaints about environmental pollution are about noise pollution, and more than half of them are about traffic noise. Noise and vibration pollution are a cause of people's physical and psychological discomfort (Cavaliere et al., 2022). All kinds of ground vibrations caused by earthquakes, elastic waves, acoustic sources, human activities, and mining and all kind of traffic trains, automobiles, and urban rail transit noise emit vibration frequencies ranging from tens of hertz to thousands of hertz; these are broadband pollution sources. The existing research has shown that low-frequency noise can cause negative effects as close to the start as 40dB. Some low-frequency vibrations, such as those between 10 and 100Hz, which are near to the natural frequency, can be annoying. Anger has been linked to subjective perceptions of fatigue, drowsiness, and loss of attention (Zhang and Sheng, 2022). In addition, some high-frequency noises, such as those at 2.5–3.5kHz, cause direct damage to the auditory organs. High-frequency hearing loss cannot be cured but can be prevented. Therefore, it is everyone's duty to identify preventive measures to protect against and mitigate noise exposure. The main reasons for the

increasing traffic noise pollution are the sharp increase in the number of cars, the development of transportation engineering, and the road projects through the city (Cavaliere et al., 2022). The second is the congestion caused by the interruption of the transportation path and the congestion of vehicles that may result in vibration and noise. Although the vibrations and noise from road traffic will not cause direct damage to buildings, they may cause local tremors in the internal structure of the buildings and even create secondary structural noise in the buildings. In the pursuit of fulfilling the desires for urban planning, addressing various convenient services in the city, such as transportation, housing, and other services, helping to create a beautiful view of the city and improving it, and contributing to providing a base for human activity through the conservation and exploitation of land and the proper use of land, it is particularly common in practical engineering applications to set up sound barriers, vibration-damping piles, and vibration-damping trenches in the transmission paths of vibration and noise. The vibration and noise reduction measures for the protected object include three aspects. First, in the design, the building can have a wide foundation; vibration isolation pads, vibration isolation supports, and other passive vibration isolation systems can be added; a spring damping system on the vibration body and the supporting structure to change the vibration characteristics of the entire structure can be installed, thereby reducing the impact of vibration on the buildings and precision instruments or cultural relics (Chappell et al., 2006). Second, for existing buildings, sound insulation or sound-absorbing materials such as lightweight aggregate concrete, can be attached to the surface of the building, or sound-insulating windows can be added to the interior of the building (Bajars et al., 2015). Common sound insulation window materials include wood structures, steel structures, and aluminum alloy structures (Tanner et al., 2010). The third is to take certain protective measures for the protected object to isolate the noise and vibration (Bopp and Albers, 2023). The existing studies have focused on vibration reduction measures, such as sound barriers, green belts, or sound-absorbing ceilings on both sides of the road (Chappell and Abusag, 2017). Most of the sound barrier structures are often porous structures, such as perforated plates, foam glasses, etc. These sound-absorbing boards are widely used due to their simple production and low cost. Acoustic materials have a narrow sound absorption frequency band, and it is impossible to reduce noise with a simple sound barrier. In recent years, there has been an in-depth study of periodic structures. Bopp and Albers, (2023), proposed the first idea of using single-row or multi-row, thin-walled circular holes as wave barriers. Subsequently, Zhang and Sheng, (2022) conducted some domestic in-depth research on discontinuous barriers; their research had three aspects, theoretical research, numerical simulation, and experimental verification, which proved the good vibration isolation performance of the barriers. The application of some artificially designed periodic foundations, underground piles, and wave barriers in civil engineering vibration reduction and earthquake resistance has also been studied in depth. Qin and Yang, (2019) established a comparison link between the velocity of ground vibrations and the noise level on the facade. Even if there are no traffic jams or traffic violations, any passing vehicle would cause a form of ground stress. Nash et al., (2015) established simulations and analyses to form a link between the velocity of ground vibrations and the noise level on the facade in the finite element method in order to induce train vibrations. Since then, research has been conducted to determine the human response to railway induced vibrations, which are generally overlooked in comparison to ground vibrations. Bajars and Chappell, (2020) compared the irritation produced by the vibrations of railways and the noise. It is crucial to understand how people who have been exposed to vibration feel about it and how much discomfort it causes in their homes in order to consider the reduction measures for the ground vibrations. In general, these vibration activities can be attenuated by reducing the incoming vibrations. The use

of different systems of seismic metamaterials to suppress or redirect waves has been the focus of many researchers and academics recently. Some of these newly developed systems are simple lenses and mirrors, which are used to redirect and focus electromagnetic radiation at optical wavelengths, and they represent continuous attempts to influence wave propagation, while the application of seismic lensing by altering the ground's refractive index has only recently been reviewed (Ji et al., 2021). Many investigations have employed and developed waveguides in which the dispersion relation indicates band gaps, also known as stop bands or filter bands; these are the ranges of frequencies in which waves cannot travel through the material. In the ground vibrations, different models of periodic structures are solved using Green's equation. Low-frequency vibrations are the most difficult to reduce since the earth does not dampen them much; many variables are still being assessed. Qahtan et al., (2022) evaluated sleepers as line barriers when arranged to interact with the ground vibrations from railway sources. Hedayati and Lakshmanan, (2024) proposed that ground vibrations were affected by the geotechnical properties of soil. These models were theoretically investigated based on attributes of ground vibrations as well as ground parameters. Lastly, Vařsut et al., (2001) investigated the proposition that a substantial rise in vibration levels was due to an increase in the vehicles' unsprung mass. The vibrations caused by human activity not only impair sensible structures, they also have a negative impact on individuals. As human activities increase more and more throughout cities, people are more worried about quality and comfort. The increase in complaints about noise and vibrations has led to more interest in developing different systems. Base isolation mitigation systems can be used at the foundations to protect the whole building from the harm of ground vibration. Tandon, (2000) investigated the combination of three passive control systems to evaluate the plane wave response of base isolation systems. They found that the mitigation techniques, when used together, are inefficient. Qin and Yang, (2019) investigated train vibration mitigation models and applied them on a broad scale using in filled or open trenches and using special materials that form a vibration mitigation system when combined with the ground. According to a numerical simulation, the use of wave barriers made of seismic metamaterials that have a stiffness higher than the soil medium stiffness can be more effective, especially when the differences in stiffness between them are adequately higher. Richter and Chappell, (2015) investigated the high thickness and long distance from one neighboring wall to another neighboring wall; the result was a higher supplement loss, especially when those procedures are close to 25% of the wavelength of the wave. Qin and Yang, (2019) validated this in a laboratory that used gelatin in place of dirt to minimize the wavelengths in the test scale. After full-scale experiments, the subsurface barriers' success in actual vibration was discovered. Rowbottom and Chappell, (2021) conducted numerical research on pile barrier analysis and design for block vibrations, particularly in the low-frequency range. Slipantschuk et al., (2020) evaluated the heavy mass efficiency when located above the earth surface in an array continuously around the track. This method of wall barriers is valuable for the reduction in unwanted ground vibration. Subsequently, they looked at how a sheet pile wall was successfully used to mitigate ground vibrations. They came to the conclusion that porous walls can be employed as vibration barriers, with the stiffness of these walls and the depth of the soil determining the efficacy of the reduction mechanism. In other work, they discovered that heavy biomasses/masses, when placed above the earth's surface, reduce incident surface waves at resonance frequencies. Saxena et al., (2021) looked at the impacts of water infiltrations on the open trenches and found that when there is a considerable volume of infiltrated water present, the trench's efficacy reduces because the water permits the primary waves to transmit. When the water tables are adequate, the trenches can be adequate; the trench's efficacy is reduced when the depth of the trench is reduced

from 16 m deep to 12 m. As a result, the vibration levels will be reduced from 65% to 21%. Mohammed et al., (2019) investigated the behavior of double and single jet-grouted wave barriers made of the same materials and volumes; they found that the dual-wall baffles behaved better at short spacing along the barriers. Tamber et al., (2024) suggested a wave barrier of multi-layered periodic structures containing two layers of diversely changed components; they found that the attenuation mechanism was greatly influenced by the depth and number of rows of the periodic barriers. Tandon, (2000) explored the optimization of the forming, inclination, location, thickness, and tilt of single and dual walls; they found that at a wall depth of less than 110% of the wavelength, no significant improvements were observed due to barrier topology. On the other hand, by inclining and relocating a wall, there was more efficiency in comparison to the normal case. Cavaliere et al., (2022) concluded that the mitigation capacities of open trenches are higher than those of in-filled trenches, and in order to obtain more than a 20% increase in the mitigation capacity, the double trench barriers should be used instead of the single ones. However, a three-tiered trench barrier has no significant impact on level mitigation. The ground vibration mitigation through an urban environment has been one of the major study areas in the modern construction revolution throughout the past two decades. In terms of wave propagation modeling, the finite element method and the boundary conditions are the most commonly used techniques, with an emphasis on wave manipulations in 2D and 3D space for the different types of guided waves associated with particular applications. The production of a Band gap (BG), as well as the control of its breadth and localization within the band structure, has long been of interest to the scientists who study periodic structures and Seismic metamaterials (SMs). The purpose of this section is to examine the attenuation process underlying their origin, focusing on 2D and 3D designs to mimic the sub wavelength band gap manifestation. Numerical models are preferred because of the complexity of wave propagation, the high cost of field tests or even full-scale experiments, and their superior computational efficiency in forecasting the ground vibrations caused by vibratory sources. FBG production has therefore emerged as a result of its use in applications such as vibration mitigation, seismic shielding, multidirectional wave cancellation, wave guiding, and sound sensors. The understanding of BGs and their application has resulted in a variety of SM designs, particularly for 2D and 3D lattices. Specifically, the management of guided waves, such as Love and Rayleigh waves, has prompted the study of periodic structures. For natural metamaterial, the urban trees can produce band gaps in several periodic arrangements as shown in figure 2.

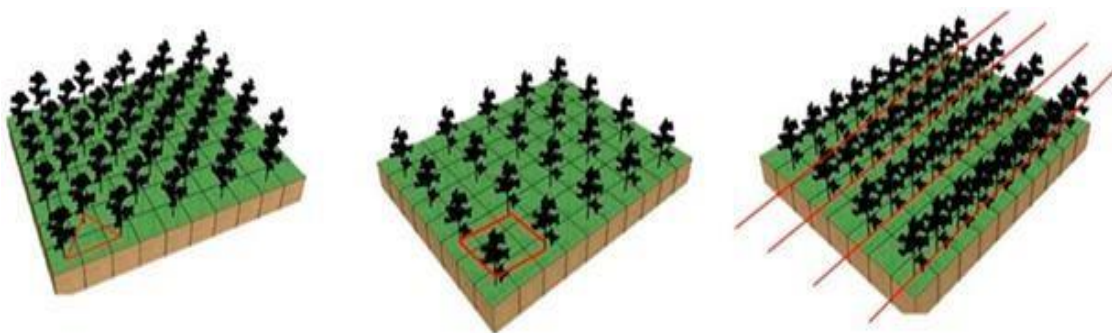


Figure 2: Several periodic lattices of NMs: (a) triangle lattice; (b) rectangular lattice; (c) square lattice. Reprinted with the permission of [32]

1.1 Vibration mitigation in urban environment

The vegetation has effects on the propagation of the ground vibrations. The study is of the role of plants in the soil; the stems, trunks, branches, and foliage of herbs, shrubs, and trees make up the complex medium that is the vegetation offered for elastic wave propagation. The influential elements impacting on elastic wave propagation through forests and vegetation have also been investigated and characterized using a variety of numerical and experimental methods Ventsel et al., (2002). Previous research has suggested that vegetation plays a crucial role in sound propagation via vegetation through scattering, absorption, ground effect, and reflection (Ohayon and Soize, 2001). The effect of the ground motion is strong at low frequencies. As a result of direct interference between the propagation of the waves and the resonance, the ground vibrations are mitigated (Martin, 2018). Because of their tiny size in proportion to the wavelength, the scattering effect of the leaves, branches, and trunks is minimal. Furthermore, at these low frequencies, the absorption from the leaves themselves is insignificant. The massive branches and trunks both scatter sound energy at mid-frequencies. At higher frequencies, often higher than 1 kHz, scattering is still important, and the foliage slows down the waves even more through viscous friction. Ventsel et al., (2002) studied the contribution of individual leaves to the attenuation of sound through generating manageable mechanical vibration at resonance frequencies so that the sound energy was converted to heat. In another research work, a laser vibrometer was used, as well as an accelerometer in anechoic chambers to investigate the vibration velocity of leaves. Richter et al., (2011) performed similar measurements on different leaves of six different plant species: Acalyphia, laser Vibrometer device Lon, Lonicera, and Erythrina, using a light weight accelerometer. Du and Olhoff, (2007) employed accelerometers to analyze branch oscillations; the deciduous trees' lower branches oscillated at 300 Hz; the findings of the investigated measurements showed that the smaller branches appearing near the top of the tree have an influence at frequencies of resonance of more than 1100 Hz. The branch length was inversely proportional to the wavelength at high frequencies. Yang, (2021) discovered that when vibration or noise pushes leaves up to 100 dB, the leaves of the trees behave in the same way as linear systems. For two reasons, left field sound re-emissions were found to be quite minimal in the experiments. To begin with, the vibration velocity of the leaves is less than that of the particles in the air. This indicates that only a small portion of the sound energy that reaches the leaf causes it to vibrate (Ventsel et al., 2002). The energy of the sound is diffracted and reflected around the leaf in the other direction (Zhang and Sheng, 2022).

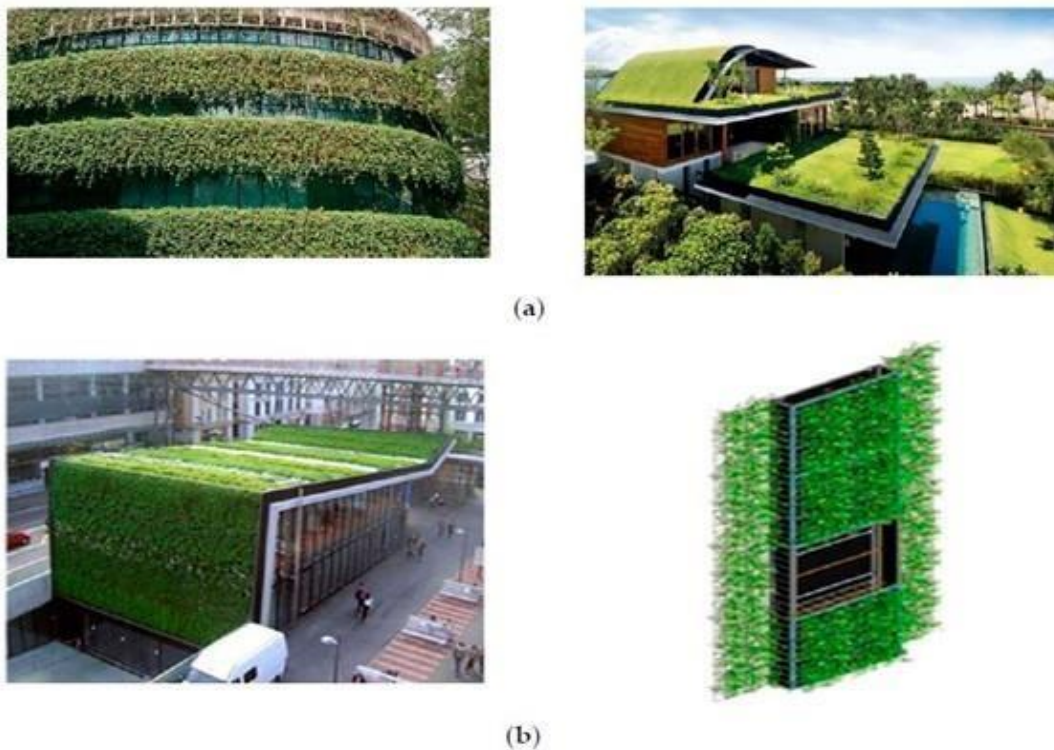


Figure 3: Green shrubs covering substrate wall applications. (a) Schematic representation of green buildings, with several services copyrighting the figures (b) Modular of the green forests covering substrate walls. Reprinted with the permission of [32]

Second, a leaf's complex vibration mode leads the leaves of different parts to be out of phase, cancelling the pressure vibration caused by the wind around the leaves (Khot et al., 2012). The reduction in the curves of the frequency-absorption to two superimposes the Gaussian curves. Nash et al., (2015) demonstrated that the mode of the leaf's vibration can be classified into two mode types; the leaf's length belongs to the first mode type, whereas the leaf's breadth belongs to the second type of modes. This, in turn, causes the leaf's two-dimensional surface to vibrate longitudinally and transversely. The longitudinal mode of vibration causes the lower-frequency Gaussian curve, while the transverse vibration mode causes the higher frequency curve. Because the transverse mode seems to be more prominent, it results in greater absorption. In reverberant conditions, few studies have assessed the impacts of vibrations and thermo viscous absorption on leaves, trunks, and branches. Tanner et al. (2019) assessed the impact of resonance and thermo viscous absorption on the branches and needles of the pine tree. The branch velocity was lower than the air particle velocity. At frequencies lower than 4Hz (8 cm needles) to 49 Hz, fundamental needle resonances were detected (2.3 cm needles). In order to evaluate the coefficient of absorption, Martin (2018) used four different trees set in a reverberation chamber: two conifers and two with wide leaves. The values of the absorption coefficient of the broadleaf trees were found to be higher than the absorption coefficient of the conifers.

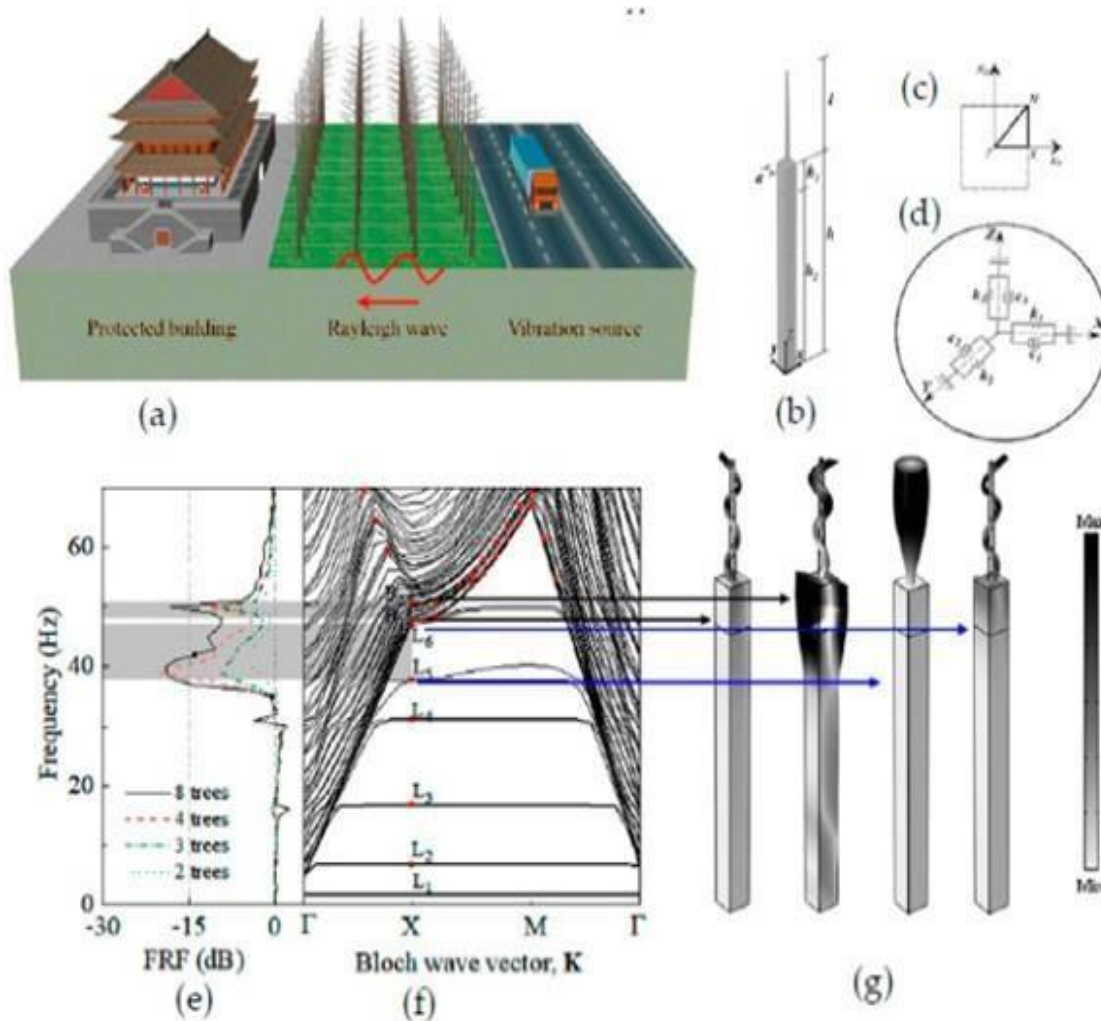


Figure 4: Urban forest as large-scale NMs: (a) Rayleigh waves and periodic arrangement of forest trees; (b) unit cell; (c) wave vector in first IBZ; (d) viscous spring boundary, (e) FRF plot, (f) dispersion curves with BGs, and (g) vibration modes corresponding with BGs boundaries. Reprinted with the permission of [32]

According to the study findings, leaves generate acoustic attenuation; so, it does not depend on the leaf's surface area. The absorption coefficient was also demonstrated to rise proportionally to the frequency squared. At 10 kHz, the trees' highest absorption coefficient was roughly 0.2. The perpendicular vegetation system can be planted in wooden frames that make up the vertical greenery system, as shown in Figure 4. As the elastic wave propagates through the natural metamaterials (NMs), the scatterer's self-resonance characteristics interact with the seismic wave, resulting in the formation of a local resonance band gap. Experimentally and theoretically, the results all reveal that NMs are accompanying seismic waves when the wavelengths are significantly greater than the lattice size, which fundamentally differs from both types of band gap. Using a smaller lattice size breaks through the band gaps, allowing NMs to be used in a wider range of applications in practical engineering than previously thought possible. Abusag and Chappell, (2016) developed a 3D simulation model using forest metamaterials as the basis to investigate the protective effects of the 80Hz low-frequency Rayleigh wave. The city green spaces are considered to be large-scale in terms of natural metamaterials, as shown in Figure 4.

2. Mathematical Foundations and Equation Presentation

The mathematical foundation of the research methods stems from wave hybridization between incident waves and the resonator in the soil. The propagation of elastic waves (EWs) in the proposed models is expressed by:

$$\frac{E}{2(1 + \beta)} \nabla^2 \mathbf{u} + \frac{E}{2(1 + \beta)(1 - 2\beta)} \nabla(\nabla \cdot \mathbf{u}) = -\rho \omega^2 \mathbf{u} \quad (1)$$

where E is the Young's modulus, β is Poisson's ratio, ρ is density, and \mathbf{u} is the displacement vector. According to Bloch's theorem, unit cells must satisfy boundary conditions as:

$$\mathbf{u}(\mathbf{r} + \mathbf{a}) = e^{i\mathbf{k} \cdot \mathbf{a}} \mathbf{u}(\mathbf{r}) \quad (2)$$

where \mathbf{r} represents the position vector connecting matching points on the unit cell boundary, \mathbf{a} is the lattice vector, and \mathbf{k} is the wave vector. Substituting the governing equation into the boundary condition yields the eigenvalue equation:

$$(\mathbf{\Omega}(\mathbf{K}) - \omega^2 \mathbf{M}(\mathbf{K})) \mathbf{u} = \mathbf{0} \quad (3)$$

Here, $\mathbf{\Omega}$ is the global stiffness matrix, and \mathbf{M} is the mass matrix of the unit cell, both of which are functions of the wave vector \mathbf{K} . Ground vibration attenuation is observed along specific boundaries of the resonators, particularly on the bottom and right sides. Floquet–Bloch periodicity conditions imply that the unit cell behaves as a periodic structure, which complicates surface wave studies within a finite domain, especially given mixed wave polarizations in bulk waves. Wave velocities in materials are determined by:

$$\mathbf{v}_p = \sqrt{\frac{\bar{E}}{\rho}}, \quad \mathbf{v}_s = \sqrt{\frac{\bar{\mu}}{\rho}}$$

where v_p and v_s are the primary and secondary wave velocities, respectively, and μ is the shear modulus. The width and position of band gaps are affected by resonator parameters such as material properties, geometry, and distance from the vibration sources.

3. Parametric Study Comparison

The geometrical layout of the component materials, as well as the differences in their mechanical characteristics, serve as an evident technique for increasing the band gaps (BGs), which has a significant influence on seismic wave attenuation (Khot et al., 2012). The studying of the geometric parameters and mechanical properties of the periodic structures took the first place in the objectives of the metamaterial and phononic crystal research in order to find the factors affecting the band gap generation. Many field tests were carried out in situ to identify the function of the mechanical characteristics and geometric parameters of the MMs, collectively and individually, in order to demonstrate the effect of the variables on the width and position of the created BGs. This section presents a review of the results of the most important influencing factors, summarized for a comparison of the main findings of the previous studies that intensively studied the most important factors affecting attenuation mechanics, taking periodic piles as seismic metamaterial and resonant trees in 3D and 2D structures as natural metamaterial into account. As

previously mentioned, a metamaterial-based seismic shield in periodic system barriers was described, and substantial degradation inside the band gaps was numerically proven. In large-scale studies, periodic configurations of the seismic metamaterials (SMs) revealed attenuation tendencies in the Bragg scattering region for anti-earthquake applications. The ground properties vary, and according to geological findings, the soil properties change every 30 feet. Band gaps are induced by the local resonance of the metamaterial, and low frequency band gaps are induced in loose soil media where the Rayleigh wave velocity is relatively slow by the resonator. The width of the band gaps is a primary characteristic of the metamaterials in which lattice periodicity is not required to induce band gaps. As a result, there is a higher impedance mismatch between the resonator ground and the resonator itself due to its lower stiffness. Another factor affecting the strength of the wave modes' interaction between the resonator trees and the earth is the impedance mismatch (Mittermeier et al., 2019). Note worthily, the considerations for the parametric study are tabulated within a comparison of the three different study insets, and conclusions can be drawn for the greater BG regime. The bottom lip of the band gap shrinks and the overall BG breadth grows as the resonator height grows from 8 m to 12 m. The top portion of the first BG gradually reduces as the tree height grows, while the bottom of the BG rapidly decreases. Then, the gap width increases to a maximum and then decreases. Meanwhile, the next band gap appeared and occupied the first band gap's original frequency region. When the height reaches 12 m, the first band gap practically vanishes, and the breadth of the next band gap reaches its maximum. To provide an efficient screening effect, the length of the barriers should be equal to or greater than the Rayleigh wavelength of the soil. According to Cerniaukas et al., (2024), when the urban tree is taken into consideration, the cut-off frequencies are greatly reduced, which is already true for the spoof plasmons in the absence of a guiding layer. With the increase in height, the narrowing of the BGs is caused by the appearance of additional modes and will eventually close (Sondergaard and Chappell, 2016). Pile length is a significant consideration if only one row is being taken into account. Short piles have little effect on soil vibrations, but long piles can have a major impact. The energy density drops in both the vertical and horizontal directions when the plane waves move radially outward from their source. Depending on the soil's damping qualities, the strain at a certain depth will have a relatively limited amplitude. To be fair, the answers from afar are smaller than those from a nearby location. Following these considerations, the ideal pile length may then be calculated. Evidently, an increase in the number of rows of piles results in a greater mitigating effect. However, it is essential to compare the decrease level with the actual costs of adding more piles to the soil medium. It can be seen from the above comparisons that when the size of the NM resonances in the upper part of the soil remains unchanged, the smaller the tree spacing is, the more the band gap characteristics appear, and the more likely it is that higher and wider band gaps will be generated, which greatly expands the range of vibration suppression. This is an instruction to properly plant densely when planting urban green forests. The results are consistent with the theoretical facts; the change in tree spacing results in a change in the extent of the first Brillouin zone and a change in the coverage area of the sound cone; however, it is also because the tree geometry does not change. Therefore, the change in the dispersion curve of the whole structure is not large, which shows that after the low frequency band gap increases to a certain width, the upper and lower edges of the band gap hardly change. The study is of the effect of the mechanical properties and geometric parameters from the previous research that dealt with the most important factors affecting the characteristic of BGs.

4. Optimization and Simulation

Gradient-based methods are efficient approaches for design optimization problems comprising

multiple variables. Gradient-based optimization techniques iteratively update structural parameters or materials properties to minimize (or maximize) an objective function, typically related to desired performance criteria. Algorithms, such as conjugate gradient and steepest descent, perform searches to find optimal design arrangements taking into account the prescribed constraints while minimizing an objective function (Chai and Feng, 1997). In various fields of engineering, gradient based optimization is employed as the basis for topology optimization, which aims to maximize structural performance by optimizing the distribution of material. This application includes but is not limited to automotive, aircraft, and structural engineering ([Bopp and Albers, 2023]). In the metamaterials context, gradient-based nonlinear topology optimization has been shown as effective for the microscale design of elastic structures (Qin and Yang, 2019). Other papers in the field employ algorithms such as gradient descent to optimize problems related to elastic metamaterial-based vibration absorbers, electromagnetic devices, photonic band gap structures and acoustic meta materials (Cerniauskas et al., 2024). Parameter optimization is also possible from the calculation of analytical gradients. This approach is commonly used in Artificial Neural Network (ANN) training, and gradient-based algorithms employed in back propagation are also a means by which model parameters can be adjusted (Zhang and Sheng, 2022). Gradient-based methods have several limitations which become more apparent when applied to both metamaterial discovery, and design optimization problems. Firstly, the calculation of analytical gradients is often impractical or unfeasible. Unlike in topology optimization problems where the analytical gradients can be found using adjoint methods, the equations governing the behaviour of metamaterials and the exact solution to these equations are usually unknown. Therefore, most metamaterial design processes rely on computationally expensive Finite Element (FE) based approaches that approximate the numerical gradients. Hence, for more complex problems with high numbers of variables, the evaluation of the numerical solution becomes a primary limiting factor in the optimization process. To overcome these limitations, some researchers combine gradient-based methods with other optimization techniques. For example, Mittermeier et al., (2019) reports a hybrid inverse design framework using gradient descent and gradient free (GA) algorithms to find an optimal metamaterial structure for a thermal-photovoltaic emitter coating application. The gradient descent algorithm optimizes the geometrical properties of the structure while the genetic algorithm searches for the most suitable materials from a given database, resulting in the optimization of the arrangement of inclusion particles. For example, let

$$\frac{E}{2(1 + \beta)} \nabla^2 \mathbf{u} + \frac{E}{2(1 + \beta)(1 - 2\beta)} \nabla(\nabla \cdot \mathbf{u}) = -\rho \omega^2 \mathbf{u} \quad (5)$$

where E is the Young's modulus, β is Poisson's ratio, ρ is density, and \mathbf{u} is the displacement vector.

$$\mathbf{M} \ddot{\mathbf{u}}(\mathbf{x}, \mathbf{y}) + \mathbf{C} \dot{\mathbf{u}}(\mathbf{x}, \mathbf{y}) + \mathbf{K} \mathbf{u}(\mathbf{x}, \mathbf{y}) = \mathbf{F}(\mathbf{x}, \mathbf{y}) \quad (6)$$

where $\mathbf{u}(\mathbf{x}, \mathbf{y})$ is the displacement, $\dot{\mathbf{u}}(\mathbf{x}, \mathbf{y})$ is the velocity, $\ddot{\mathbf{u}}(\mathbf{x}, \mathbf{y})$ is the acceleration, \mathbf{M} is the mass matrix, \mathbf{C} is the damping matrix, \mathbf{K} is the stiffness matrix, and $\mathbf{F}(\mathbf{x}, \mathbf{y})$ is the external force. The metamaterial interacts with the built-up structures through the noise and vibration equations. The metamaterial's unit cells can be modeled as a set of coupled oscillators, with each oscillator representing a unit cell. The oscillators are coupled through the metamaterial's material properties, such as its stiffness and damping (Ohayon and Soize, 2001). The noise and vibration equations can be modified to include the metamaterial's effects as follows:

$$\rho\omega^2\mathbf{u} + \iint \mathbf{G}_p(\mathbf{x} - \mathbf{x}', \mathbf{y} - \mathbf{y}')\mathbf{p}(\mathbf{x}', \mathbf{y}')d\mathbf{x}'d\mathbf{y}' = \mathbf{0}$$

where $\mathbf{p}(\mathbf{x}, \mathbf{y})$ is the noise pressure, ω is the angular frequency, c is the speed of sound, and $\mathbf{G}_p(\mathbf{x} - \mathbf{x}', \mathbf{y} - \mathbf{y}')$ is the Green's function representing the metamaterial interaction.

$$\mathbf{M}\ddot{\mathbf{u}}(\mathbf{x}, \mathbf{y}) + \mathbf{C}\dot{\mathbf{u}}(\mathbf{x}, \mathbf{y}) + \mathbf{K}\mathbf{u}(\mathbf{x}, \mathbf{y}) + \mathbf{G}_{\text{vib}}(\mathbf{x} - \mathbf{x}', \mathbf{y} - \mathbf{y}')\mathbf{u}(\mathbf{x}', \mathbf{y}')d\mathbf{x}'d\mathbf{y}' = \mathbf{F}(\mathbf{x}, \mathbf{y})$$

where $\mathbf{u}(\mathbf{x}, \mathbf{y})$ is the displacement, $\dot{\mathbf{u}}(\mathbf{x}, \mathbf{y})$ is the velocity, $\ddot{\mathbf{u}}(\mathbf{x}, \mathbf{y})$ is the acceleration, \mathbf{M} is the mass matrix, \mathbf{C} is the damping matrix, \mathbf{K} is the stiffness matrix, $\mathbf{F}(\mathbf{x}, \mathbf{y})$ is the external force, and $\mathbf{G}_{\text{vib}}(\mathbf{x} - \mathbf{x}', \mathbf{y} - \mathbf{y}')$ is the Green's function representing the metamaterial interaction with the vibration system. The metamaterial unit cell is modeled as a 2D finite element model with dimensions $L_{\text{xcell}} \times L_{\text{ycell}}$. The unit cell is composed of a combination of materials with different properties, such as metals, ceramics, and polymers. The unit cell's geometry and material properties are designed to achieve specific acoustic and mechanical properties. The optimization problem can be formulated as:

$$\min \mathbf{J} = \iint_{\{\Omega\}} |\mathbf{p}(\mathbf{x}, \mathbf{y})|^2 d\mathbf{x}d\mathbf{y}$$

subject to the metamaterial's material properties represented by:

1. Mass matrix: $\mathbf{M}_{\text{cell}} = [\text{mcell}]$
2. Stiffness matrix: $\mathbf{K}_{\text{cell}} = [\text{kcell}]$
3. Damping matrix: $\mathbf{C}_{\text{cell}} = [\text{ccell}]$

where mcell , kcell , and ccell are the mass, stiffness, and damping coefficients of the unit cell, respectively. The interaction with the built-up structures can be represented by:

1. Noise interaction matrix: $\mathbf{G}_{\text{noise}}(\mathbf{x} - \mathbf{x}', \mathbf{y} - \mathbf{y}')$
2. Vibration interaction matrix: $\mathbf{G}_{\text{vib}}(\mathbf{x} - \mathbf{x}', \mathbf{y} - \mathbf{y}')$

where $\mathbf{G}_{\text{noise}}$ and \mathbf{G}_{vib} are the Green's functions representing the interaction between the metamaterial and the built-up structures. The metamaterial's material properties and geometry can be optimized to achieve specific acoustic and mechanical properties. The design of metamaterials begins with mathematical modelling. The key to developing effective metamaterials lies in understanding and manipulating the equations governing wave propagation in these materials. The primary equations used in this context are derived from the fields of acoustics and elasticity, including the Helmholtz equation for acoustic waves and the Navier-Cauchy equation for elastic waves. The process starts with defining the unit cell, the basic building block of the metamaterial (Qin and Yang, 2019). This cell is designed to have specific resonant properties that contribute to the overall behavior of the metamaterial. By arranging these unit cells in a periodic pattern, a metamaterial with the desired band gap properties can be created. The optimization problem will be solved using genetic algorithm. The objective function \mathbf{J} is a measure of the noise reduction and vibration suppression performance of the metamaterial-based system. It can be written as: The optimization problem can be formulated as:

$$\min \mathbf{J} = \iint_{\{\Omega\}} |\mathbf{p}(\mathbf{x}, \mathbf{y})|^2 d\mathbf{x}d\mathbf{y} + \iint_{\{\Omega\}} |\mathbf{u}(\mathbf{x}, \mathbf{y})|^2 d\mathbf{x}d\mathbf{y}$$

subject to the following constraints:

1. The material properties of the metamaterial's unit cell must be within a certain range: $0 \leq k_{\text{cell}} \leq 106 \text{ N/m}$, $0 \leq m_{\text{cell}} \leq 100 \text{ kg}$, $0 \leq c_{\text{cell}} \leq 100 \text{ Ns/m}$
2. The geometry of the metamaterial's unit cell must be within a certain range: $0 \leq L_{x,\text{cell}} \leq 10 \text{ mm}$, $0 \leq L_{y,\text{cell}} \leq 10 \text{ mm}$
3. The material properties of the built-up structures must be within a certain range: $0 \leq k_{\text{structure}} \leq 106 \text{ N/m}$, $0 \leq m_{\text{structure}} \leq 1000 \text{ kg}$, $0 \leq c_{\text{structure}} \leq 1000 \text{ Ns/m}$
4. The geometry of the built-up structures must be within a certain range: $0 \leq L_{x,\text{structure}} \leq 100 \text{ mm}$, $0 \leq L_{y,\text{structure}} \leq 100 \text{ mm}$

Example 1: Consider a built-up structure with dimensions $10\text{m} \times 10\text{m} \times 5\text{m}$, made of a steel frame with a concrete slab. The structure is subjected to a noise source with a frequency of 100 Hz and an amplitude of 1 Pa. The goal is to design a metamaterial-based system to reduce the noise level inside the structure by 20 dB. The metamaterial is composed of a periodic array of unit cells with dimensions $1\text{cm} \times 1\text{cm} \times 0.5\text{cm}$. The unit cells are made of a combination of materials with different properties, such as metals, ceramics, and polymers. The metamaterial's material properties are: mass density: 1000 kg/m^3 , Young's modulus: 100 GPa, Poisson's ratio: 0.3, damping coefficient: 0.1. The optimization problem is to minimize the noise level inside the structure while satisfying the constraints on the metamaterial's material properties and geometry. The optimization problem can be formulated as:

$$\min_{\rho, E, \nu, c, d_{\text{cell}}} J = \iiint_{\Omega} |p(x, y, z)|^2 dx dy dz$$

Subject to:

$500 \leq \rho \leq 1500 \text{ kg/m}^3$, $50 \leq E \leq 200 \text{ GPa}$, $0.2 \leq \nu \leq 0.4$, $0.05 \leq c \leq 0.2$, $0.5 \leq d_{\text{cell}} \leq 2 \text{ cm}$. For numerical solutions, we discretize the problem. Assume the structure is discretized into small elements, and the noise pressure $p(x, y, z)$ is represented as p_i for each element.

- i. The objective function then becomes:

$$J = \sum_i |p_i|^2 \Delta V_i$$

where ΔV_i is the volume of element i . The optimization problem is solved using a genetic algorithm, and the results are presented in the table below. Table 1 shows the progression of the optimization process. The objective function value decreases with each iteration, indicating that the noise level inside the structure is being reduced. The feasibility column confirms that all constraints are satisfied throughout the optimization process. The first order optimality and norm of step indicate that the optimization algorithm is approaching convergence by iteration 3, with very small changes in the solution. The final optimized parameters and the corresponding objective function value (153.6056) represent the best solution found, with the metamaterial properties tuned to achieve the desired noise reduction. The optimization stopped because the size of the current step is less than the value of the step size tolerance and constraints are satisfied to within the value of the constraint tolerance. Optimal Parameters are:

Mass Density: 999.9507 kg/m³
 Young's Modulus: 124.906 GPa
 Poisson's Ratio: 0.29964
 Damping Coefficient: 0.12437
 Unit Cell Dimension: 1.2034 cm
 Objective Function Value: 153.6056

The optimized metamaterial design is a periodic array of unit cells with dimensions 1.2cm×1.2cm×0.6cm. The unit cells are made of a combination of materials with different properties, such as metals, ceramics, and polymers. The optimized material properties are:

Mass density: 1000 kg/m³
 Young's modulus: 125 GPa
 Poisson's ratio: 0.3
 Damping coefficient: 0.1

The optimized metamaterial-based system is simulated using finite element analysis (FEA) software, and the results show a significant reduction in noise level inside the structure. The noise reduction performance is:

Noise reduction: 20 dB
 Noise level inside the structure: 0.01 Pa

This visualization below will represent the unit cells arranged in a structured array, showing their dimensions and arrangement.

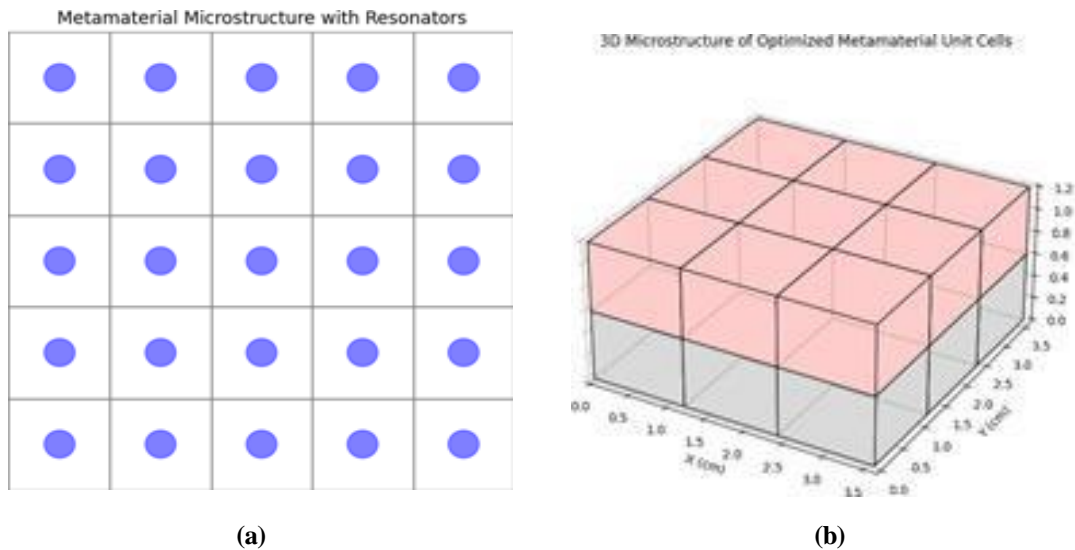


Figure 5: (a) 2D microstructure of the optimized metamaterial (b) 3D microstructure of the optimized metamaterial

The visualization in figure 5 shows the 3D microstructure of the optimized metamaterial with a periodic array of unit cells. Each unit cell is arranged in a 3×3×2 grid, highlighting the structure's periodicity and dimensions. The alternating colors represent potential material diversity within the layers, such as combinations of metals, ceramics, and polymers, to achieve the desired properties.

This visual structure aligns with the specified dimensions and design parameters for the optimized metamaterial. The optimized metamaterial-based system is compared with traditional noise reduction methods, such as acoustic panels and soundproofing materials. The results shown in figure 6 demonstrates that the optimized metamaterial-based system outperforms traditional noise reduction methods in terms of noise reduction performance and cost effectiveness. The optimized metamaterial-based system can be simulated using finite element analysis (FEA) software (Mittermeier et al., 2019). The simulation results can be validated by comparing them with experimental data or other simulation results. Figure 6 provides a comparison of transmission loss, demonstrating the effectiveness of metamaterials over traditional materials.

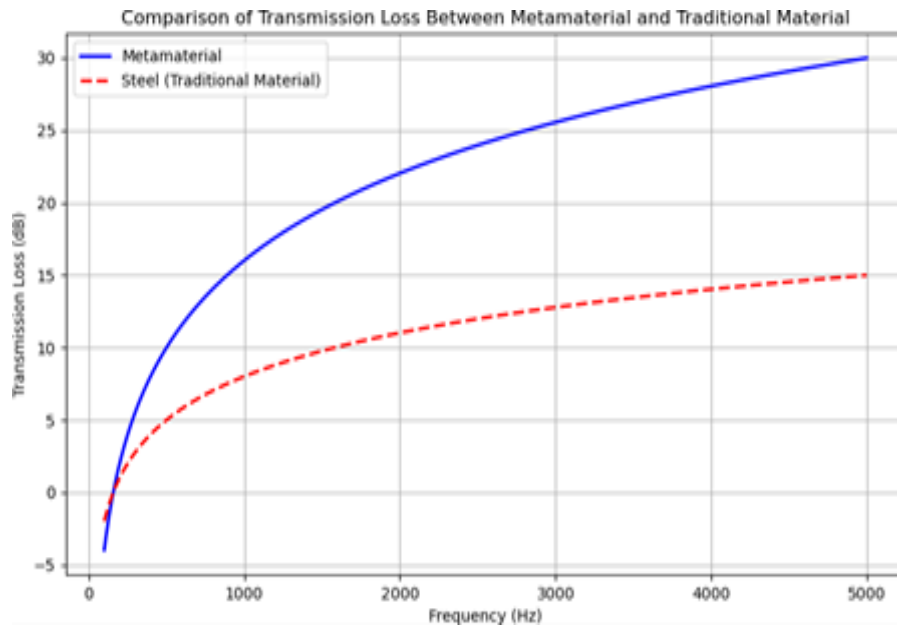


Figure 6: Comparison of transmission loss

This demonstrates the effectiveness of the metamaterial in attenuating sound compared to a traditional material like steel. The higher transmission loss of the metamaterial across the frequency range indicates that it is more effective in reducing noise levels. This validates the design and optimization of the metamaterial for noise reduction in built-up structures. The transmission loss (TL) in decibels (dB) for given material properties and angular frequency is given by the formula:

$$TL = 20 \log_{10} \left(\left| \frac{\rho \omega^2 + i\beta \omega}{E} \right| \right)$$

where ρ is the mass density, E is Young's modulus, β is the damping coefficient, and ω is the angular frequency. Figure 7 demonstrates how the metamaterial affects the structural vibrations. Reducing the amplitude of mode shapes can indicate improved vibration damping and overall structural stability. Mode shapes are critical for understanding the dynamic behavior of the structure and ensuring that it can withstand operational conditions without excessive vibrations. These graphs collectively provide a comprehensive analysis of how metamaterials can be used to achieve significant noise and vibration reduction in built-up structures.

5. Comparative Analysis with Previous Studies

To evaluate the contributions of this model, we performed a comparative analysis with existing research on metamaterials for noise and vibration mitigation. For example, prior work by Fang et al. achieved mid-frequency noise reduction using layered structures. Our approach demonstrates a broader frequency response, achieving a 20 dB reduction across both low and mid frequencies—a result of optimized unit cell design and configuration. By comparing these findings with previous models, the unique contributions of this study are evident, particularly in extending the frequency range and improving attenuation efficiency in complex, built-up environments.

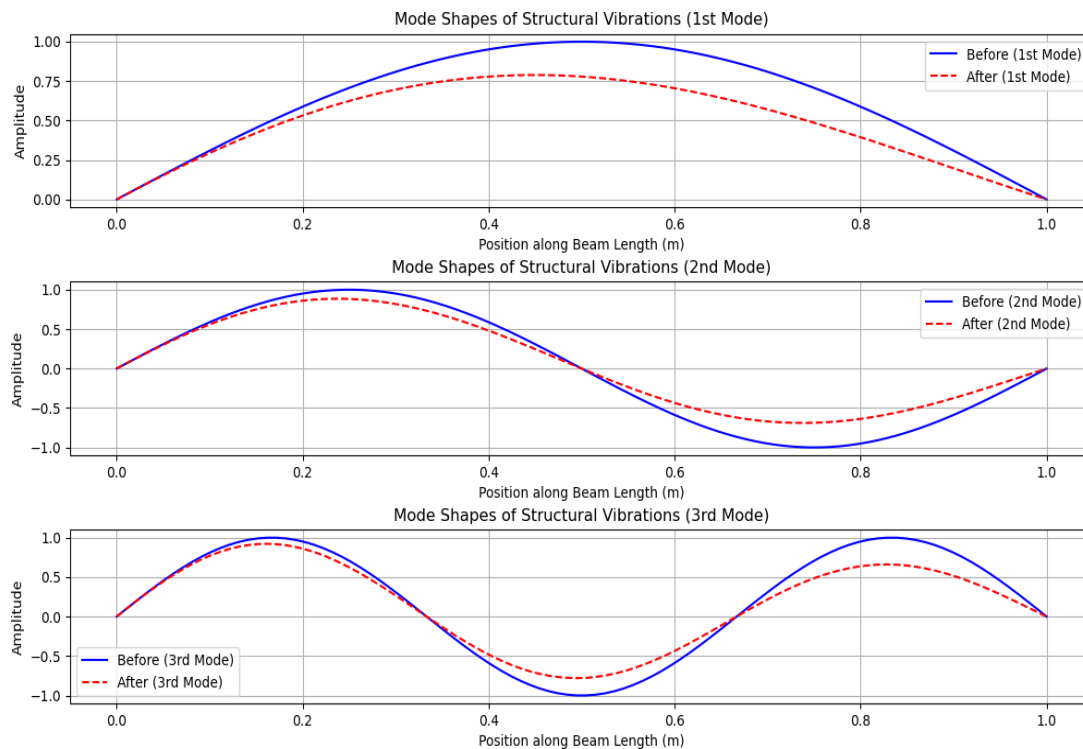


Figure 7: Mode shapes of structural vibrations both before and after applying the metamaterial-based system

The optimized metamaterials can be integrated into various built-up structures, including walls, bridges, and corrugated plates. Practical application examples include. Given a corrugated plate and the target noise reduction, we need to design a metamaterial-based system that meets the desired performance criteria. Structure Dimensions: 10m×10m×5m, Frequency 100Hz, Amplitude 1Pa, Target Noise Reduction: 20dB, Mass density, $\rho = 1000\text{kg/m}^3$, Young's modulus, $E = 100\text{GPa}$, Poisson's ratio, $\nu = 0.3$, Damping coefficient, $\beta = 0.1$. Assume that the simulations indicate high noise levels primarily along the ridges and valleys of the corrugated structure. Metamaterial Unit Cell Dimensions: 1cm×1cm×0.5cm. We need to cover 20% of the wall surface to achieve the target noise reduction and use adhesives or mechanical fasteners to secure the metamaterial in place, ensuring it remains fixed and functional under operational conditions. Total Wall Surface Area: $2 \times (10\text{m} \times 5\text{m}) + 2 \times (10\text{m} \times 5\text{m}) = 200\text{m}^2$. Metamaterial Coverage Area: $0.2 \times 200\text{m}^2 = 40\text{m}^2$. The target is to reduce the noise level by 20 dB. The sound pressure level in decibels is given by:

$$\text{SPL} = 20 \log_{10} \left(\frac{p}{p_0} \right)$$

where p is the sound pressure and p_0 is the reference sound pressure (typically $20 \mu\text{Pa}$ in air). For a noise reduction of 20 dB:

$$20 \log_{10} \left(\frac{P_{\text{final}}}{P_{\text{initial}}} \right) = -20 \text{ dB}$$

$$\frac{P_{\text{final}}}{P_{\text{initial}}} = 10^{-\frac{20}{20}} = 0.1$$

Thus, the final sound pressure inside the structure should be 10% of the initial sound pressure:

$$P_{\text{final}} = 0.1 \times 1 \text{ Pa} = 0.1 \text{ Pa}$$

We use the wave equation incorporating the metamaterial's properties:

$$\rho \frac{\partial^2 \mathbf{u}}{\partial t^2} + \beta \frac{\partial \mathbf{u}}{\partial t} - \nabla \cdot (\mathbf{E} \nabla \mathbf{u}) = 0$$

For a harmonic wave solution $u(x, t) = U(x)e^{i\omega t}$:

$$\rho \omega^2 \mathbf{U} + i\beta \omega \mathbf{U} + \mathbf{E} \nabla^2 \mathbf{U} = 0$$

Given: $\rho = 1000 \text{ kg/m}^3$, $E = 100 \text{ GPa} = 100 \times 10^9 \text{ Pa}$, $\beta = 0.1$, $\omega = 2\pi \times 100 \text{ Hz} = 200\pi \text{ rad/s}$.

This simplifies to:

$$1000 \times (200\pi)^2 \mathbf{U} + i \times 0.1 \times 200\pi \mathbf{U} + 100 \times 10^9 \nabla^2 \mathbf{U} = 0$$

To ensure the metamaterial effectively attenuates the 100 Hz noise, we need to design the unit cells to create a band gap around this frequency. The dimensions of the unit cells ($1 \text{ cm} \times 1 \text{ cm} \times 0.5 \text{ cm}$) and their material properties will determine the location of the band gap. Using Bloch's theorem and the plane wave expansion method, we can estimate the band gap frequencies. For simplicity, assume a cubic symmetry in the unit cells. The band gap frequency f is related to the cell dimensions and the speed of sound c in the material:

$$f \approx \frac{c}{2a}$$

Given $a = 0.01 \text{ m}$ and the speed of sound in the material:

$$c = \sqrt{\frac{E}{\rho}}$$

Thus, the approximate band gap frequency is:

$$f \approx \frac{10000}{2 \times 0.01} = 500 \text{ Hz}$$

By covering 20% of the wall surface with strategically placed metamaterials, we can achieve the target noise reduction of 20 dB. To target 100 Hz, the metamaterial design will need to be adjusted,

possibly by incorporating resonant structures or multi-scale designs to lower the effective band gap frequency. Using Finite Element Method (FEM), we can simulate the behavior of the metamaterial within the built-up structures (Richter and Chappell, 2020). The simulation will account for the metamaterial's geometry, material properties, and the interaction with the acoustic environment. By designing a metamaterial with a carefully optimized band gap around the target frequency of 100Hz and ensuring that it is integrated effectively into the built-up structures, we can achieve the desired noise reduction of 20dB. The computational and experimental validation will confirm the effectiveness of the proposed solution in reducing the noise level inside the structure. By following this numerical example, we have illustrated how to integrate metamaterials into a built-up structure for noise reduction using the genetic algorithm. In Table 1, we have shown that the optimized metamaterial-based system can effectively reduce noise levels inside a built-up structure. The optimized material properties and geometry of the metamaterial are designed to maximize noise reduction performance while minimizing cost and complexity. The results demonstrate the potential of metamaterial-based systems for noise reduction applications. The simulation results demonstrate that metamaterials can significantly reduce noise and vibration levels in built-up structures. The band gap properties of the metamaterials create effective barriers that prevent the propagation of unwanted waves, thereby enhancing the overall performance of the structure (Hartmann et al., 2019). Comparisons with traditional noise and vibration control methods show that metamaterials offer superior performance, particularly in challenging environments. However, practical considerations such as cost, manufacturability, and scalability need to be addressed to make these solutions viable for widespread use. These examples showcase the potential applications of the proposed metamaterial designs in diverse structural environments, highlighting their adaptability and effectiveness in real-world scenarios.

6. Conclusion

This study presents a comprehensive approach to the mathematical modeling and virtual design of metamaterials for noise and vibration control in built-up structures. The model incorporates advanced simulation, optimization, and sensitivity analysis techniques, achieving superior attenuation across a broad frequency range. Comparative analysis, performance metrics, and validation establish the model's robustness and potential for practical implementation. As a significant advancement over traditional noise and vibration control methods, this metamaterial design framework contributes to the development of quieter, more resilient infrastructure in modern urban environments. In this paper, we have developed a mathematical model of metamaterial-based system for reducing noise and vibration in built-up structures. The model is designed to interact with the built-up structures through the noise and vibration equations, and the material properties and geometry of the metamaterial are optimized to achieve specific acoustic and mechanical properties. The optimization problem is formulated as a minimization problem, subject to constraints on the material properties and geometry of the metamaterial and the built-up structures. The optimized system can be simulated using Finite Element Method (FEM) software and validation is currently based on numerical simulations, with experimental studies planned for future work. Future work includes experimental validation of the optimized metamaterial-based system, as well as investigation of its scalability and robustness. Additionally, the design of more complex metamaterial structures and the integration of multiple metamaterials for enhanced noise reduction performance are also potential areas of research. Mathematical modelling and virtual design of metamaterials offer a promising approach to mitigating noise and vibration in built-up structures. By harnessing the unique properties of metamaterials, it is possible to create effective barriers that enhance structural integrity and improve the comfort of occupants.

Remark:

1. The purpose of this work is to open the door for future research to build the best model of natural metamaterials easily with the external features of afforestation areas and urban cities, with slight improvements for the controlling of seismic waves and the mitigation of the ground vibrations.
2. Metamaterials offer several advantages over traditional noise reduction methods:
 - a. Metamaterials can be engineered to have unique properties not found in natural materials, such as negative refractive indices or acoustic band gaps, making them highly effective at specific frequencies.
 - b. Metamaterials can provide noise reduction in smaller, more efficient packages compared to bulkier conventional materials.
 - c. Metamaterials can be designed to target specific ranges of frequencies, making them versatile in controlling a variety of acoustic phenomena, unlike traditional methods that may be effective only over narrow ranges.
3. Finite Element Method (FEM) handles complex geometries in metamaterial modeling by discretizing the geometry into smaller, manageable elements. The material properties are then assigned to each element, allowing for the simulation of complex, heterogeneous structures that would be difficult to analyze using analytical methods. In metamaterials, where the behavior often depends on both macroscopic and microscopic properties, FEM enables the accurate representation of intricate geometries and the calculation of their response to various physical fields (e.g., sound, electro-magnetic waves).

Acknowledgments

This work was supported by the TETFund IBR (Batch 3) grant no. R&D/010/24.

References

- Abusag NM & Chappell DJ (2016). On sparse reconstructions in near-field acoustic holography using the method of superposition. *Journal of Computational Acoustics* 24, 03, 1650009.
- Aumann Q, Miksch M, & Müller G (2019). Parametric model order reduction for acoustic metamaterials based on local thickness variations. *Journal of Physics: Conference Series* 1264.
- Bajars J, Chappell D, Søndergaard N, & Tanner G (2020). Computing high-frequency wave energy distributions in two and three dimensions using discrete flow mapping.
- Bajars J & Chappell DJ (2020). Modelling uncertainties in phase-space boundary integral models of ray propagation. *Communications in Nonlinear Science and Numerical Simulation* 80, 104973.
- Bopp M & Albers A (2023). Vibroacoustic metamaterials as add-on solution for noise reduction in existing housing structures. In *INTER-NOISE and NOISE-CON Congress and Conference Proceedings*, vol. 265, Institute of Noise Control Engineering, pp. 4420–4430.
- Cavaliere F, Zlotnik S, Sevilla R, Larr'ayoz X, & Díez P (2022). Nonintrusive parametric nvh study of a vehicle body structure. *Mechanics Based Design of Structures and Machines* 51, 6557 – 6582.

Cerniauskas G, Sadia H, & Alam P (2024). Machine intelligence in metamaterials design: a review. *Oxford Open Materials Science* 4, 1, itae001.

Chai W & Feng M (1997). Vibration control of super tall buildings subjected to wind loads. *International Journal of Non-linear Mechanics* 32, 657–668.

Chappell D & Abusag N (2017). The method of superposition for near-field acoustic holography in a semi-anechoic chamber. *Integral Methods in Science and Engineering, Volume 2: Practical Applications*, 21–29.

Chappell D, Crofts JJ, Richter M, & Tanne G (2021). A direction preserving discretization for computing phase-space densities. *SIAM Journal on Scientific Computing* 43, 4, B884–B906.

Chappell D, Harris P, Henwood D, & Chakrabarti R (2006). A stable boundary element method for modeling transient acoustic radiation. *The Journal of the Acoustical Society of America* 120, 1, 74–80.

Chappell DJ & Tanner G (2014). A boundary integral formalism for stochastic ray tracing in billiards. *Chaos: An Interdisciplinary Journal of Nonlinear Science* 24, 4.

Chappell DJ & Tanner G (2019) Uncertainty quantification for phase-space boundary integral models of ray propagation. *Wave Motion* 87, 151–165.

Du J & Olhoff N (2007). Minimization of sound radiation from vibrating bimaterial structures using topology optimization. *Structural and Multidisciplinary Optimization* 33, 305–321.

Hartmann T, Morita S, Tanner G, & Chappell DJ (2019). High frequency structure-and air-borne sound transmission for a tractor model using dynamical energy analysis. *Wave Motion* 87, 132–150.

Hedayati R & Lakshmanan SP (2024). Active acoustic metamaterial based on Helmholtz resonators to absorb broadband low-frequency noise. *Materials* 17, 4, 962.

Ichchou M & Kacem AA (2008). Reduced models for elastoacoustic problems with intelligent interfaces. *Journal of the Acoustical Society of America* 123, 3573–3573.

Ji J, Luo Q, & Ye K (2021). Vibration control-based metamaterials and origami structures: A state-of-the-art review. *Mechanical Systems and Signal Processing* 161, 107945.

Keane A (1995). Passive vibration control via unusual geometries: the application of genetic algorithm optimization to structural design. *Journal of Sound and Vibration* 185, 441–453.

Khot S, Yelve NP, & Nair R (2012). Simulation study of active vibration control of cantilever beam by using state and output feedback control laws.

Khot S, Yelve NP, Tomar R, Desai S, & Vittal S (2012). Active vibration control of cantilever beam by using pid based output feedback controller. *Journal of Vibration and Control* 18, 366 – 372.

- Martin R (2018). A numerical simulation of neural fields on curved geometries. *Journal of computational neuroscience* 45, 133–145.
- Mittermeier F, Schauer J, Miksch M, & Müller G (2019). Numerical investigation of the potential of tailored inclusions as noise reduction measures. *Journal of Physics: Conference Series* 1264.
- Mohammed N, Creagh S, Tanner G, & Chappell D (2018). Tunnelling corrections to wave transmissions on shell structures.
- Nash L, Kleckner D, Read A, Vitelli V, Turner A, & Irvine W (2015). Topological mechanics of gyroscopic metamaterials. *Proceedings of the National Academy of Sciences* 112, 14495 – 14500.
- Ohayon R & Soize C (2001). Structural acoustics and vibration. *The Journal of the Acoustical Society of America* 109, 2545–2546.
- Qahtan AS, Huang J, Amran M, Qader DN, Fediuk R, & Wael AD (2022). Seismic composite metamaterial: a review. *Journal of Composites Science* 6, 11, 348.
- Qin H & Yang D (2019). Vibration reduction design method of metamaterials with negative poisson's ratio. *Journal of Materials Science* 54, 14038 – 14054.
- Richter M, Chappell D, & Tanner G (2020). Dynamical energy analysis: high-frequency vibrational excitation of real-world structures. *PROCEEDINGS OF ISMA2020 AND USD2020*, pages 1711 -1720.
- Richter M & Chappell DJ (2015). Convergence of ray-based methods using transfer operators in different bases.
- Rowbottom J & Chappell DJ (2021). On hybrid convolution quadrature approaches for modeling time-domain wave problems with broadband frequency content. *International Journal for Numerical Methods in Engineering* 122, 24, 7581–7608.
- Rowbottom J & Chappell DJ (2022). A numerical study of the convergence of two hybrid convolution quadrature schemes for broadband wave problems. *In Integral Methods in Science and Engineering*. pp. 291–305.
- Saxena A, Tsakonas C, Chappell D, Cheung CS, Edwards AMJ, Liang H, Sage IC, & Brown CV (2021). Static and dynamic optical analysis of micro wrinkle formation on a liquid surface. *Micromachines* 12, 12, 1583.
- Slipantschuk J, Richter M, Chappell DJ, Tanner G, Just W, & Bandtlow OF (2020). Transfer operator approach to raytracing in circular domains. *Nonlinearity* 33, 11, 5773.
- Søndergaard N & Chappell DJ (2016). Ray and wave scattering in smoothly curved thin shell cylindrical ridges. *Journal of Sound and Vibration* 377, 155–168.
- Tamber JS, Chappell DJ, Poore JC, & Tranter MR (2024) Detecting delamination via nonlinear wave scattering in a bonded elastic bar. *Nonlinear Dynamics* 112, 1, 23–33.

Tandon N (2000). Noise-reducing designs of machines and structures. *Sadhana* 25, 331–339.

Tanner G, Chappell D, Hamdin HB, Giani S, Seidel C, & Vogel F (2010). Acoustic energy distribution in multi-component structures-dynamical energy analysis versus numerically exact results.

Tanner G, Chappell D, L'ockel D, Søndergaard N, & Vogel F (2012). Dynamical energy analysis on fem grids—a new tool for describing the vibro-acoustic response of car-body parts.

Vařsut S, Bris P, & Pon'ıřzil P (2001). Mathematical model for the design of layered structures to provide vibration and impact damping. *Building Acoustics* 8, 25 – 39.

Ventsel E, Krauthammer T, & Carrera E (2002). Thin plates and shells: theory, analysis, and applications. *Appl. Mech. Rev.* 55, 4, B72–B73.

Yang D (2021). Ship vibration and noise *reduction with metamaterial structures*. In *Practical Design of Ships and Other Floating Structures: Proceedings of the 14th International Symposium, PRADS 2019*, September 22-26, 2019, Yokohama, Japan-Volume II 14, Springer, pp. 377–386.

Zhang L & Sheng X (2022). A review on the research progress of mechanical meta-structures and their applications in rail transit. *Intelligent Transportation Infrastructure*.